SENSOR PERFORMANCE OF CANTILEVERED MAGNETOSTRICTIVE BEAM

Cao Qinghua[1, 2, 3], Chen Dingfang[2], Lu Quanguo[3], Tang gang[3], Yan Jianwu[3], Zhu Zhifang[3], Xu Bin[3], Zhao Ran[3], Zhang Xiaoxing[3]

1, School of Automation, Wuhan University of Technology, Wuhan, China

2, Institute of Intelligent Manufacturing and Control, Wuhan University of Technology, Wuhan, China

3, Institute of Micro/nano Actuation and Control, Nanchang Institute of Technology, Nanchang, China

Email: qh9863@126.com[1]; cadcs@126.com[2]

Submitted: Mar. 30, 2014 ***Accepted: July 15, 2014*** ***Published: Sep. 1, 2014***

Abstract- A nonlinear couple modeling of magnetostrictive cantilever is built by combining Gibb's free energy formulation with the Euler-Bernoulli beam theory. The Gibb's free energy corresponding to different orientations in 3D space can be expressed in terms of their direction cosines, the stress at a given point can be described by classical theory. The magnetomechanical bending experimental setup is designed. The results demonstrated magnetostrictive sensing can be performed in bending even when both tensile and compressive stresses are developed; meanwhile the sensing is primarily due to the dominating effect of compression over tension.

Index terms: Magnetostrictive, beam, nonlinear couple, sensor performance

I. INTRODUCTION

Smart materials can transduce one form of energy to another, and the energy transduction is manifested as a change in shape and physical properties of the materials when they are exposed to an external energy field which produces a change in their atomic arrangement. Such changes are used in actuator and sensor applications. They show the different effects related to energy transduction between electrical, magnetic, mechanical andthermal fields. The more widely smart materials such as piezoelectric, magnetostrictive and shape memory alloy (SMA) are used. These materials are grouped together due to certain common physical and functional characteristics shared by them, Piezoelectric materials offer several advantages such as large blocked stress (~50 MPa) and free strain ($\sim 1000\mu\varepsilon$), fast response as they are activated by electric field (voltage) with an operational bandwidth of upto 20 MHz and low impedance at high frequencies.but require very high electric field (voltage) and are brittle and extremely sensitive to temperature which restricts them from being used in harsh environments. Due to the absence of a spontaneous polarization, electrostrictives can be used as a sensor only.

Piezoelectric materials are used in a variety of actuator and sensor applications [1, 2, 3]. They are widely used in several transducers like accelerometers, load cells and pressure sensors. Engineered piezoelectric transducers such as RAINBOW and THUNDER are used in valves, linear motors, configurable mirrors and synthetic jet actuators. Other aerospace applications include active control of twist and flap in rotor blades and development of configurable airfoils. Piezoelectric stacks are also used in ultrasonic motors, sonars and for nano-positioning in AFM and STM stages. In the presence of a bias electric field, SMA [2, 4, 5] such as Nitinol ($Ni_{55}Ti_{45}$) exists in a low temperature martensite phase and a high temperature austenite phase which can be reversibly obtained by cycling temperature. But they are brittle and their bandwidth is limited by eddy current formation.

Magnetostrictive materials such as Terfenol-D show high strain and blocked stress [6, 7]. In general, all magnetostrictives show fast response as magnetic field can be controlled by changing current which can be changed as fast as electric field. Unlike piezoelectric, these materials can be used under static and low frequency conditions with very low impedance but they offer high impedance at high frequencies (kHz range) due to the inductive nature of the materials. One of

the reasons for the promise of these materials in a host of applications is the development of a new class of structural magnetostrictive materials, iron–gallium alloys (Galfenol).

Galfenol exhibits moderate magnetostriction (~350 ppm) under very low magnetic fields ~100Oe, have very low hysteresis, and demonstrate high tensile strength (~500 MPa) and limited variation in magnetomechanical properties for temperatures between −20°C and 80°C. These materials are, in general, machinable, ductile and can be welded. Thus, they can be easily threaded, attached to existing structures and used as load bearing members. They have a high Curie temperature (675 °C) and are corrosion resistant. The raw materials used to produce Galfenol are relatively inexpensive. All these factors demonstrate that Fe-Ga alloys have great promise as an engineering material for actuation and sensing applications [8, 9, 10].

Yoo designed a tuning fork-based gyro sensor which uses mm-size Galfenol patches as actuator and sensor material in bending. Downey showed that mm-scale Galfenol rods can be used as a sensor in bending and the results of this work was used to conceptualize a nanowire-based broadband acoustic sensor. Further work in this area led to the mechanical characterization of Galfenol nanowires which showed that although their Young's modulus is similar to that of bulk material, they possess almost three times the tensile strength. Datta and Flatau showed that Galfenol could be adhered to a structural material and used as strain sensor in bending. Hale and Flatau and Parsons demonstrated the application of Galfenol in tactile sensing and torque sensing respectively. Ghodsi developed a positioning actuator for cryogenic environment. Ueno et al. developed linear actuator, wobblers and vibrator [11, 12, 13].

Such applications motivate the development of a modeling framework and performance analysis for active structures. Structural modeling of extensional magnetostrictive transducers has successfully been performed, while performance analysis of Magnetostrictive cantilever has been a challenge.

Various non-linear models have also been developed to account for the magnetomechanical response of ferromagnetic materials over different operating conditions. Higher order series expansion of the free energy yielded the Landau model. Bergqvist and Engdahl combined the effects due to stress and magnetic field into an equivalent field term and incorporated this in the Preisach operator to model the effect of stress on magnetization [14]. A stress-induced field term was introduced into the Langevin term by Jiles to model the effect of stress on magnetization vs. field curves as well as the effect of magnetic field on magnetization vs. stress curves. Ghosh and

Gopalakrishnan used a neural network technique to non-linearize the coupled constitutive equations and successfully predicted both the actuation and sensing characteristics of magnetostrictive materials. These models were limited to one-dimensional analysis and did not account for magnetocrystalline anisotropy which is required to capture the directional preference of magnetization orientation based on the crystal symmetry of different materials.

Armstrong [15] extended the Stoner-Wohlfarth model to cubic anisotropy and was able to come up with a three-dimensional model for magnetostrictive actuation. This approach was adapted to model both the actuator and predict the sensor responses of single crystal and polycrystalline Galfenol subjected to collinear stress and magnetic fields. An extension to this approach was developed to add stress-annealing effect by incorporating a uniaxial anisotropy. These models included Zeeman, stress-induced anisotropy and magnetocrystalline anisotropy energy but excluded the exchange energy because it is non-zero only within the domain wall and hence forms a small fraction of the total energy of a bulk sample. Moreover, the preclusion of the magnetostatic energy incapacitates the ability of these models to account for demagnetization effects.

Smith developed a homogenized energy model which included magnetostatic, stress-induced anisotropy, magnetocrystalline anisotropy and exchange energy terms [16, 17, 18, 19]. The exchange interaction was phenomenologically incorporated using Boltzmann statistics which ironically considers only noninteracting particles. Moreover the use of Boltzmann statistics is only applicable to a large number of particles and may not be a valid assumption near saturation when the material is almost in a single domain state. Using Armstrong's energy formulation and Smith's framework of homogenized energy model, Dapino developed a magnetomechanical model which takes into account six possible directions of magnetization orientation instead of two directions in Smith's work [20]. These approaches introduce dynamic effects into the constitutive model using thermal relaxation techniques and are particularly useful for obtaining closed minor loops when operating an actuator or sensor with DC bias magnetic field and stress respectively.

This article investigates the performance analysis of Galfenol-driven cantilever beam considering the effect of the magnetic induction and stress. In order to motivate a modeling technique in the frame, a magnetostrictive cantilever beam model is established, constitutive relations that describe the material behavior are based on energy minimization techniques. The saturation

magnetization (M_s), the magnetostrictive constant (λ_{100}) and the 4th and 6th order anisotropy constants (K_1 and K_2 respectively) are used to calculate the Zeeman, stress-induced anisotropy and magnetocrystalline anisotropy energies per unit volume. The Euler-Bernoulli assumption of the classical beam theory is adopted to solve stress of the magnetostrictive cantilever beam. Experiments and simulations are conducted to study performance of the cantilever.

II. MODELING OF CONSTITUTIVE BEHAVIOR

Constitutive relations that describe the material behavior are usually based on energy minimization techniques. The first part of such a technique involves the formulation of an energy functional which includes or precludes certain terms based on assumptions appropriate for the purpose of the model. The second part involves the use of mathematical techniques to extract the information about a required physical response of the material under the influence of force fields that perturb the energy.

The simplest model for magnetoelastic material is the coupled linear constitutive equations. Considering both strain and magnetic induction in the material as functions of stress and magnetic field, a first order truncated Taylor series expansion about a given operating point (H_0, σ_0) can be written as Equations (1) and (2). Note that stress and magnetic field are assumed to be independent inputs to the material.

$$d\varepsilon = \left.\frac{\partial \varepsilon}{\partial \sigma}\right|_{H_0,\sigma_0} d\sigma + \left.\frac{\partial \varepsilon}{\partial H}\right|_{H_0,\sigma_0} dH \qquad (1)$$

$$dB = \left.\frac{\partial B}{\partial \sigma}\right|_{H_0,\sigma_0} d\sigma + \left.\frac{\partial B}{\partial H}\right|_{H_0,\sigma_0} dH \qquad (2)$$

The total workdone (dW) on a unit volume of ferromagnetic material by a stress and magnetic field due to infinitesimal change in strain and magnetic induction can be expressed by Equation (3). Note that dW is not an exact differential.

$$dW = \sigma d\varepsilon + HdB \qquad (3)$$

For a reversible process, the change in internal energy (dU) can be expressed using Equation (4) which can be obtained by substituting Equation (3) in the 1st Law of Thermodynamics. Here S and T denote entropy and temperature respectively.

$$dU = \sigma d\varepsilon + HdB + TdS \quad (4)$$

The Gibb's free energy of the system is given by Equation (5)

$$G = U - \sigma\varepsilon - HB - TS \quad (5)$$

The change in Gibb's free energy in an isothermal reversible process can be expressed by Equation (6).

$$dG = dU - \varepsilon d\sigma - \sigma d\varepsilon - BdH - HdB - TdS \quad (6)$$

Combining Equations (4) and (6), the change in Gibb's free energy can be written as shown in Equation (7).

$$dG = -\varepsilon d\sigma - BdH \quad (7)$$

Equation (7) can be used to interpret the differential quantities in Equations (1) and (2) as follows. The mechanical compliance of the material in a process where the magnetic field (H_0) is maintained constant while the stress is quasistatically perturbed about a given stress σ_0 is expressed by Equation (8).

$$\left.\frac{\partial\varepsilon}{\partial\sigma}\right|_{H_0,\sigma_0} = -\left.\frac{\partial^2 G}{\partial\sigma^2}\right|_{H_0,\sigma_0} = S^{H_0,\sigma_0} \quad (8)$$

Similarly, magnetic permeability of the material in a process where the stress σ_0 is maintained constant while the magnetic field is quasi-statically perturbed about a given field (H_0) is expressed by Equation (9).

$$\left.\frac{\partial B}{\partial H}\right|_{H_0,\sigma_0} = -\left.\frac{\partial^2 G}{\partial H^2}\right|_{H_0,\sigma_0} = \mu^{H_0,\sigma_0} \quad (9)$$

The strain coefficient ($d = \partial\varepsilon/\partial H$) and stress sensitivity ($d^* = \partial B/\partial\sigma$) which couple the effects of magnetic field and mechanical stress are expressed by Equations (10) and (11) respectively and are identical to each other as evident from their relation to the 2nd derivative of the Gibb's free energy.

$$\left.\frac{\partial\varepsilon}{\partial H}\right|_{H_0,\sigma_0} = -\left.\frac{\partial^2 G}{\partial\sigma\partial H}\right|_{H_0,\sigma_0} = d^{H_0,\sigma_0} \quad (10)$$

$$\left.\frac{\partial B}{\partial \sigma}\right|_{H_0,\sigma_0} = -\left.\frac{\partial^2 G}{\partial \sigma \partial H}\right|_{H_0,\sigma_0} = d^{*H_0,\sigma_0} \quad (11)$$

The saturation magnetization (M_s), the magnetostrictive constant (λ_{100}) and the 4th and 6th order anisotropy constants (K_1 and K_2 respectively) is used to calculate the Zeeman, stress-induced anisotropy and magnetocrystalline anisotropy energies per unit volume due to a stress (σ) and a magnetic field (H) applied along the [100] direction as shown in Equations (12), (13) and (14) respectively.

$$E_H = -\mu_0 M_s H \alpha_1 \quad (12)$$

$$E_\sigma = -\frac{3}{2}\lambda_{100}\sigma\alpha_1^2 \quad (13)$$

$$E_{an} = K_1\left(\alpha_1^2\alpha_2^2 + \alpha_2^2\alpha_3^2 + \alpha_3^2\alpha_1^2\right) + K_2\left(\alpha_1^2\alpha_2^2\alpha_3^2\right) \quad (14)$$

The free energy (E_{TOT}) of the system corresponding to different orientations in 3D space can be expressed in terms of their direction cosines ($\alpha_1, \alpha_2, \alpha_3$) as shown in Equation (15).

$$E_{TOT}(\varphi,\theta) = E_H + E_\sigma + E_{an} \quad (15)$$

In order to develop an expression for the bulk magnetization and magnetostriction, it is necessary to understand the following probabilistic approach. Let us assume that a bulk magnetic material is composed of a number of noninteracting magnetization units. The fraction of these units at a state (i, j), which is defined by the orientation (φ_i, θ_j) of these units, may be denoted by p_{ij}. From the physics of ferromagnetism, a larger number of magnetic moments would align along a direction of lower energy. Since p_{ij} is proportional to the number of magnetic moments and inversely proportional to $E_{TOT}(\varphi_i, \theta_j)$, a probability density function given by Equation (16) can be used to express p_{ij} as a function of $E_{TOT}(\varphi_i, \theta_j)$. The choice of an exponential distribution in Equation (16) is made to avoid a singularity at E_{TOT} =0.

$$p_{ij}(\varphi_i,\theta_j) = N_m \exp\left[\frac{-E_{TOT}(\varphi_i,\theta_j)}{\Omega}\right] \quad (16)$$

Here N_m is a normalizing factor which can be calculated from Equation (17) from the definition of a probability density function and Ω is an empirical scaling factor. It is assumed that the energy is distributed in a sphere of unit radius.

$$N_m = \frac{1}{\int_{\varphi=0}^{2\pi}\int_{\theta=0}^{\pi} \exp\left[\frac{-E_{TOT}}{\Omega}\right]\left|\sin\theta\right| d\theta d\varphi} \tag{17}$$

Let us assume $Q(\varphi,\theta)$ is a distributed physical quantity. The expected value $\langle Q\rangle$ can be obtained from Equation (18).

$$\langle Q\rangle = \frac{\int_{\varphi=0}^{2\pi}\int_{\theta=0}^{\pi} Q(\varphi,\theta)\exp\left[\frac{-E_{TOT}}{\Omega}\right]\left|\sin\theta\right| d\theta d\varphi}{\int_{\varphi=0}^{2\pi}\int_{\theta=0}^{\pi} \exp\left[\frac{-E_{TOT}}{\Omega}\right]\left|\sin\theta\right| d\theta d\varphi} \tag{18}$$

In order to calculate the magnetization along [100], we substitute $Q(\varphi,\theta)$ with $M_{[100]}(=M_s\alpha_1)$ in Equation (18) and convert the definite integrals to finite summations which give us Equation (19). An optimum value of $\Delta\varphi = \Delta\theta = 5^0$ is used for all cases to get converged solutions in reasonable computation time.

$$M = \frac{\sum_{\varphi=0}^{2\pi}\sum_{\theta=0}^{\pi} M_s\alpha_1\left|\sin\theta\right|\Delta\theta\Delta\varphi\exp\left(\frac{-E_{TOT}}{\Omega}\right)}{\sum_{\varphi=0}^{2\pi}\sum_{\theta=0}^{\pi}\left|\sin\theta\right|\Delta\theta\Delta\varphi\exp\left(\frac{-E_{TOT}}{\Omega}\right)} \tag{19}$$

The magnetic induction is calculated using Equation (20).

$$B = \mu_0(M + H) \tag{20}$$

The same hypothesis can be extended to calculate the magnetostriction along [100] using Equation (21).

$$\lambda = \frac{\sum_{\varphi=0}^{2\pi}\sum_{\theta=0}^{\pi}\frac{3}{2}\lambda_{100}\left(\alpha_1^2 - \frac{1}{3}\right)\left|\sin\theta\right|\Delta\theta\Delta\varphi\exp\left(\frac{-E_{TOT}}{\Omega}\right)}{\sum_{\varphi=0}^{2\pi}\sum_{\theta=0}^{\pi}\left|\sin\theta\right|\Delta\theta\Delta\varphi\exp\left(\frac{-E_{TOT}}{\Omega}\right)} \tag{21}$$

The total strain can be described by Equation (22) where ES is the purely mechanical Young's modulus of the material and is also known as the modulus at magnetic saturation. This is the modulus measured when all the magnetic moments are oriented either parallel or anti-parallel.

$$\varepsilon = \frac{\sigma}{E_s} + \lambda \qquad (22)$$

III. CLASSICAL BEAM THEORY

Structural members subjected to transverse loads and operating in flexural mode are known as beams. The Euler-Bernoulli assumptions of the classical beam theory are as follows:

1. The cross-section of the beam has a longitudinal plane of symmetry known as the neutral plane.
2. The resultant of the transversely applied loads lies in the longitudinal plane of symmetry.
3. Plane sections originally perpendicular to the longitudinal axis of the beam remain plane and perpendicular to the longitudinal axis after bending.
4. In the deformed beam, the planes of cross-sections have a common intersection, that is, any line originally parallel to the longitudinal axis of the beam becomes an arc of a circle described by the radius of curvature.

These assumptions are applicable to a beam whose length is 8-10 times more than both its width and its thickness.

Figure 1. An Euler-Bernoulli beam in a Cartesian coordinate system

Let us assume a beam with length (L) along the x-direction and thickness (t) along the z-direction as shown in Figure 1, is subjected to a bending force. If the transverse displacement (w) along the z-direction after the bending deformation is much smaller than the beam thickness, then the axial displacement (u) along the xdirection can be expressed using Equation (23).

$$u = -z\frac{dw}{dx} \qquad (23)$$

The axial strain (ε_x) can be expressed using Equation (24)

$$\varepsilon_x = \frac{du}{dx} = -z\frac{d^2w}{dx^2} \qquad (24)$$

Using Equation (24) along with the constitutive equation ($\sigma_x = E\varepsilon_x$) for elastic material (where E is the Young's modulus of the beam material), a moment balance about the y-axis would yield Equation (25) which describes the relationship between bending moment (M), stress and beam dimensions.

$$\sigma_x = -z\frac{M}{I} \qquad (25)$$

In Equation (35), I is the 2nd moment of area which can be calculated from Equation (26) for a beam with a uniform rectangular cross-section as shown in Figure 1.

$$I = \int_{y=-\frac{b}{2}}^{y=\frac{b}{2}} \int_{z=-\frac{t}{2}}^{z=\frac{t}{2}} z^2 dzdy = \frac{1}{12}bt^3 \qquad (26)$$

The question posed at the end of the previous section motivates the study of the distribution of stress and magnetic induction along the thickness of a magnetostrictive beam which is fixed at x = 0 and free at x = L. A beam with these boundary conditions is also known as a cantilevered beam. Cantilevered beams are often used for bending characterization.

The stress at a given point in a cantilevered beam subjected to a transverse tip loading (F) can be described using Equation (27) which can be obtained by substituting $M = F(L-x)$ in Equation (25).

$$\sigma_x(x,z) = -z\frac{F(L-x)}{I} = -\frac{12FL}{bt^2}\left(\frac{z}{t}\right)\left(1-\frac{x}{L}\right) \qquad (27)$$

IV. EXPERIMENT RESULT AND DISCUSSION

The magnetomechanical bending experimental setup was designed. The test setup consists of magnetic and mechanical components. The magnetic components were designed to apply different DC bias magnetic fields along the length of the Galfenol beam.

Figure 2 shows the free-body diagram of the Galfenol beam specimen placed between the top and bottom fixtures. The four silicon carbide rods form line contacts with the beam which can be described by four points. The two upper rods which are separated by a distance (2a) apply equal loads of magnitude (P/2). The two lower rods which are separated by a distance (4a) provide equal reaction forces of magnitude (-P/2).

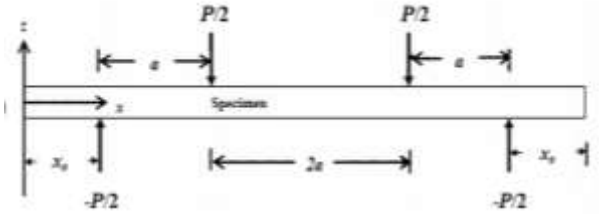

Figure 2. Free body diagram of the cantilevered beam

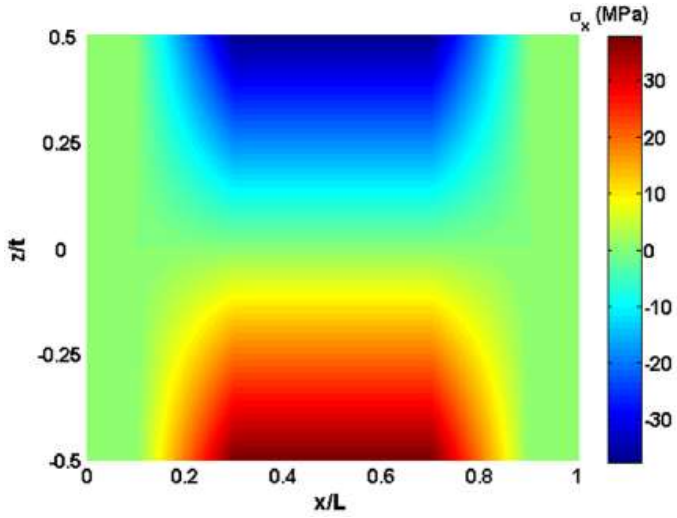

Figure 3. Stress distribution in a beam subjected to four-point bending

Figure 3 shows the stress distribution in a beam of length $25mm$ and crosssection $2mm \times 2mm$ subjected to four-point bending. A force (P) of $20N$ was used for simulation. a region of

constant stress can be seen in Figure 2 for $0.3 \le x/L \le 0.7$. A value of $x_0 = 2.5mm$ and $a = 5mm$ were used in the simulation to be consistent with the actual design.

Figure 4. The experimental set-up

Figure 4 shows the assembled test setup , the mechanical fixture was mounted on a hydraulic MTS810 universal testing machine. A silicon carbide ball that was used to transfer load from the MTS machine to the mechanical fixture provided a point contact in order to ensure that only axial force is exerted on the Galfenol beam. The electromagnet was clamped on two sides and placed in the same horizontal plane as the sample so as to apply magnetic field along the length of the sample. The DC bias magnetic field was applied by passing a constant current through the solenoid. The load was quasi-statically cycled once from 0 to 50 N at a ramp rate of 2.5 mm/min. At the end of the load cycle, the constant current in the solenoid was switched off. Before each test, the sample was demagnetized over 167 cycles using a 1 Hz sinusoidal field which underwent a 10 % geometric decay every 1.5 cycles from initial amplitude of 15 kA/m. The procedure repeated for applied magnetic fields of 0, 1.35 ± 0.1, 1.99 ± 0.5, 2.71 ± 0.5, 7.52 ± 5 and 11.01 ± 0.5 kA/m which were obtained by passing currents of 0, 0.05, 0.15, 0.25, 1 and 1.75 ampere through the solenoid.

Note that these applied magnetic fields were measured in air by placing a hand-held gaussmeter in between the pole pieces of the electromagnet for different constant current in the solenoid. In this experiment, the bias magnetic field in the sample could not be maintained during the loading cycle using the feedback controller because of the lack of closed magnetic circuit. Moreover, the stress distribution in the Galfenol beam creates a spatial distribution of the magnetic field in the beam unlike in the Galfenol rod, where a uniform stress-state in the entire rod ensured a uniform change in reluctance and magnetic field in the Galfenol sample.

A pick-up coil with 100 turns wrapped around the sample and connected to an integrating fluxmeter measured the thickness-averaged magnetic induction along the beam span between the load applicators.

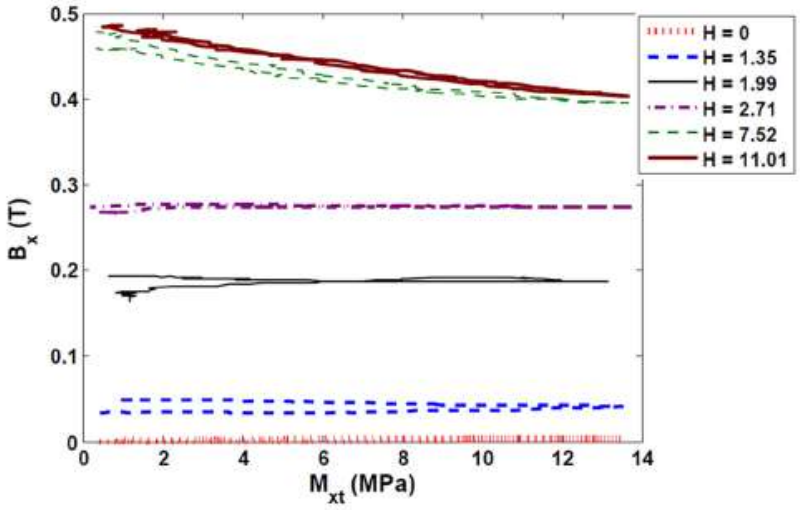

Figure 5. Thickness-averaged magnetic induction as a function of M_{xt}

Figure 5 shows the thickness-averaged magnetic induction measured by the pick-up coil placed in the mid-section of the beam in between the load application points. The maximum induction that could be observed in the Galfenol sample was limited to ~0.5T because of the following reason. An applied magnetic field of 7.52kA/m was sufficient to saturate the electromagnet steel core and hence any additional current through the solenoid did not significantly increase the flux through the electromagnet. Although the electromagnet was useful for concentrating the magnetic flux into the Galfenol sample, the lack of a perfectly closed magnetic circuit caused significant flux leakage and could generate a magnetic induction of only 0.5T in the Galfenol sample while the electromagnet core got saturated.

At a given non-zero magnetic bias field (H), Galfenol is expected to show an increase in B under tension and a decrease in B under compression. If the effect of tension and compression due to bending on B were equal then B should remain constant at all M_{xt}. Such behavior is observed at zero and low H (upto 2.71kA/m). At higher H (7.52 and 11.01kA/m), the magnetic moments are mostly aligned in the direction of H and hence a tensile stress collinear to H does not contribute to any change in B and the magnetic response is dominated by compressive stress. This is evident from the decrease in B. If M_{xt} is increased to a critical value, the magnetic moments in the

compressive region of the sample are all aligned perpendicular to H. Beyond this M_{xt}, no stress induced change in magnetic moment orientation takes place thereby leading to a steady value of B.

The thickness-averaged B can be deduced using the principle of superposition.The net B measured by the pick-up coil can be assumed to be the average of the B below the neutral axis of the Galfenol beam which is in tension and the B above the neutral axis of the beam which is in compression. The B below and above the neutral axis will be proportional to the volume fraction of magnetic moments and their orientation in these regions respectively. This information can be qualitatively deduced from the energy maps shown in Figures 5

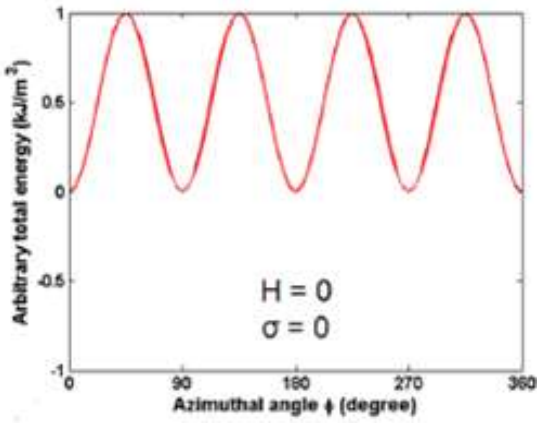

(a) In a demagnetized and un-stressed sample

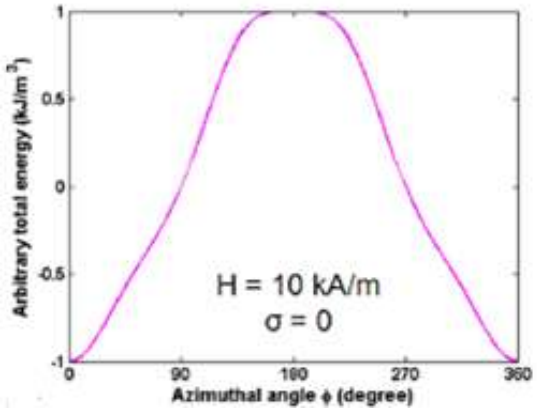

(b) After applying a high bias magnetic field

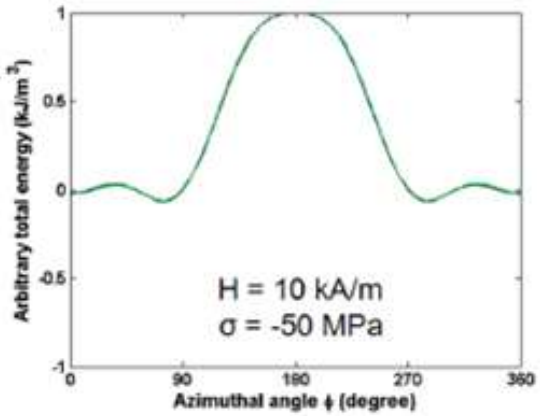

(c) In the region above neutral axis after bending

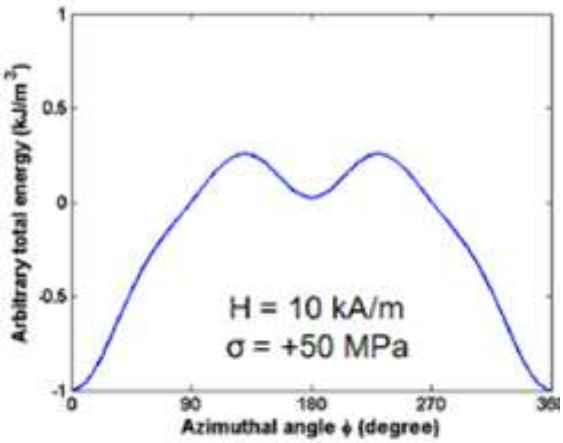

(d) In the region below neutral axis after bending.

Figure 6. Total energy distribution in the azimuthal plane

Figure 6(a) shows the four equal energy minima in Galfenol in the absence of stress and magnetic field owing to its cubic magnetocrystalline anisotropy. Figure 6(b) shows that when a large bias magnetic field is applied along 0^0, most of the magnetic moments which were earlier oriented along 90^0,180^0 and 270^0 rotate towards 0^0.When the Galfenol sample undergoes bending in presence of the large bias field, the parts of it which are in compression and tension have the energy distribution as shown in Figure 6(c) and Figure 6(d) respectively. The compressive stress rotates some of the magnetic moments lying above the neutral axis of the beam from 0^0 toward 90^0 and 270^0. The tensile stress can rotate the magnetic moments lying below the neutral axis of the beam to either 0^0 or180^0. Since most of the magnetic moments are already oriented along 0^0 under the influence of a large bias field, the tensile stress has no effect. As a result, the effect of

compressive stress in the upper half of the beam dominates over the effect of tensile stress in the beam's lower half, and a net change in thickness-averaged B is observed before and after bending in the presence of a large bias magnetic field.

VI. CONCLUSIONS

This article investigates the performance analysis of Galfenol-driven cantilever beam. A magnetostrictive cantilever beam model is established; constitutive relations that describe the material behavior based on energy minimization techniques. The Euler-Bernoulli assumptions of the Classical Beam Theory are used to solve stress of the magnetostrictive beam. Experiments and simulations are conducted to study performance of the cantilever; the sensing is primarily due to the dominating effect of compression over tension.

ACKNOWLEDGEMENT

The authors would like to acknowledge the financial support by the National Natural Science Fund of China (Grant No. 51165035, 51175395and 51161019), and Youth Science Fund of Jiangxi province office of education of China (Grant No.GJJ11247). Guangxi Key Laboratory of Manufacturing System & Advanced Manufacturing Technology (Grant No. 11-031-12S05), MoE Key Laboratory of Metallurgical Equipment，Their Control (Grant No. 2013B09) and the Youth Science Fund of Jiangxi Province (20114BAB216006).

REFERENCES

[1] J. Abbaszadeh, H. Abdul Rahim, E. Najafiaghdam, R. Abdul Rahim and S. Sarrafi, "INCREASING THE EFFICIENCY OF ULTRASONIC DISPERSION SYSTEM WITH USE OF CONTROL LOOP TO AUTOMATIC FREQUENCY ADJUSTING", International Journal on Smart Sensing and Intelligent Systems, vol. 4, No.2, 2011, pp. 205-223.

[2] K. B. Waghulde and Dr. Bimlesh Kumar, "Vibration Analysis of Cantilever Smart Structure by using Piezoelectric Smart Material", vol. 4, No.3, pp.2011, pp. 353-375.

[3] B.Biju, N.Ganesan and K.Shankar, "TRANSIENT DYNAMIC BEHAVIOR OF TWO PHASE MAGNETO-ELECTRO-ELASTIC SENSORS BONDED TO ELASTIC RECTANGULAR PLATES", vol. 5, NO.3, 2012, pp. 645-672.

[4] A.Yousaf, F.A.Khan and Prof. Dr. L.M Reindl, "Wireless sensing of open loop micro inductors using Helmholtz coil", International Journal on Smart Sensing and Intelligent Systems.vol. 4, NO.4, 2011, pp. 527-546.

[5] I. Chopra, "Review of State of Art of Smart Structures and Integrated Systems", AIAA Journal, vol. 40, NO.11, 2002, pp. 2145-2187.

[6] Dapino, M.J, Smith, R.C. and Flatau, A.B. "A Coupled Structural- Magnetic Strain Model for Magnetostrictive Transducers", Journal of Intelligent Material Systems and Structures, vol. 11, February 2000, pp.545-556.

[7] D. C. Jiles, "Theory of the magnetomechanical effect", Journal of Physics D:Applied Physics, vol. 28, NO.8, 1995, pp. 1537-1546.

[8] D. P. Ghosh and S. Gopalakrishnan, "Role of Coupling Terms in Constitutive Relationships of Magnetostrictive Materials", Computers, Materials and Continua,vol. 1, NO.1, 2004, pp. 213-227.

[9] J.Atulasimha and A. B Flatau, "A review of magnetostrictive iron–gallium alloys", Smart Mater, Struct. vol. 20, 2011, pp.1-15.

[10] J. Atulasimha, G. Akhras, and A. B. Flatau, "Comprehensive three dimensional hysteretic magnetomechanical model and its validation with experimental <110> single-crystal iron-gallium behavior", Journal of Applied Physics, vol. 103, No.7, 2008, pp. 07B336.

[11] Jayaraman T V, "Srisukhumbowornchai N, Guruswamy S and Free M L .Corrosion studies of single crystals of iron–gallium alloys in aqueous environments", Corrosion Science, vol. 103, NO.10, 2007, pp.4015–4027.

[12] J. B. Restorff, M. Wun-Fogle, A. E. Clark, and K. B. Hathaway, "Induced Magnetic Anisotropy in Stress-Annealed Galfenol Alloys, Magnetics", IEEE Transactions on, vol. 42, NO.10, 2006, pp. 3087-3089.

[13] J.-H. Yoo, U. Marschner, and A. B. Flatau, "Preliminary Galfenol vibratory gyro-sensor design in Smart Structures and Integrated Systems", San Diego, CA, Proc. of SPIE, Vol. 5764, March 2005. pp. 111-119.

[14] P. G. Evans and M. J. Dapino, "State-Space Constitutive Model for Magnetization and Magnetostriction of Galfenol Alloys,Magnetics", IEEE Transactions on, vol. 44, NO.7, pp. 2008. 1711-1720.

[15] P. R. Downey and A. B. Flatau," Magnetoelastic bending of Galfenol for sensor applications, Journal of Applied Physics", Proc. of SPIE Vol. 6174,2006.pp.0B1-9.

[16] R. C. Smith, M. J. Dapino, T. R. Braun, and A. P. Mortensen, "A homogenized energy framework for ferromagnetic hysteresis", Magnetics, IEEE Transactions on, vol. 42, NO.7, 2006, pp. 1747-1769.

[17] S.Datta and A. B. Flatau, "Magnetostrictive Vibration Sensor based on Iron-Gallium Alloy" Proc. of MRS, Vol.888 , 2005, pp.4-9.

[18] T. Ueno and T. Higuchi, "Miniature Magnetostrictive Linear Actuator Based On Smooth Impact Drive Mechanism", International Journal of Applied Electromagnetics and Mechanics, vol. 28, 2008. pp. 135-141.

[19] W. D. Armstrong, “A directional magnetization potential based model of magnetoelastic hysteresis”, Journal of Applied Physics, vol. 91, NO.4,2002,pp. 2202-2210.
[20] Liang Shu, Leon M Headings, et al, “Nonlinear model for Galfenol cantilevered unimorphs considering full magneto elastic coupling”, Journal of Intelligent Material Systems and Structures , July 2013,pp.1-17.